

Passivation of Si nanocrystals in SiO₂ : Atomic versus molecular hydrogen

A. R. Wilkinson and R. G. Elliman

Citation: *Applied Physics Letters* **83**, 5512 (2003); doi: 10.1063/1.1637130

View online: <http://dx.doi.org/10.1063/1.1637130>

View Table of Contents: <http://scitation.aip.org/content/aip/journal/apl/83/26?ver=pdfcov>

Published by the [AIP Publishing](#)

Articles you may be interested in

[Passivation effects in B doped self-assembled Si nanocrystals](#)

Appl. Phys. Lett. **105**, 222108 (2014); 10.1063/1.4903776

[A low thermal impact annealing process for SiO₂-embedded Si nanocrystals with optimized interface quality](#)

J. Appl. Phys. **115**, 134311 (2014); 10.1063/1.4870819

[Donor ionization in size controlled silicon nanocrystals: The transition from defect passivation to free electron generation](#)

J. Appl. Phys. **113**, 024304 (2013); 10.1063/1.4772947

[Influence of surface chemistry on photoluminescence from deuterium-passivated silicon nanocrystals](#)

J. Appl. Phys. **106**, 063121 (2009); 10.1063/1.3224952

[Elucidation of the surface passivation role on the photoluminescence emission yield of silicon nanocrystals embedded in SiO₂](#)

Appl. Phys. Lett. **80**, 1637 (2002); 10.1063/1.1456970

The advertisement features a photograph of the Model PS-100 cryogenic probe station, which is a complex piece of scientific equipment with various mechanical components and a probe. The background is a gradient of blue and white. The text is arranged around the image, with the product name and description on the left, the company logo on the right, and a slogan at the bottom right.

Model PS-100
Tabletop Cryogenic
Probe Station

The logo for Lake Shore CRYOTRONICS consists of a stylized blue and white square icon to the left of the company name. 'Lake Shore' is in a large, white, serif font, and 'CRYOTRONICS' is in a smaller, white, sans-serif font below it.

Lake Shore
CRYOTRONICS

*An affordable solution for
a wide range of research*

Passivation of Si nanocrystals in SiO₂: Atomic versus molecular hydrogen

A. R. Wilkinson^{a)} and R. G. Elliman

Department of Electronic Materials Engineering, Research School of Physical Sciences and Engineering,
The Australian National University, Canberra, ACT, 0200, Australia

(Received 22 July 2003; accepted 5 November 2003)

Photoluminescence measurements were used to investigate the effect of atomic and molecular hydrogen on the passivation of Si nanocrystals in SiO₂. Significant increases in the luminescence intensity and lifetime were found in samples coated with a thin Al layer prior to a standard anneal in molecular hydrogen. This is shown to be consistent with enhanced passivation of the nanocrystals by atomic hydrogen. © 2003 American Institute of Physics. [DOI: 10.1063/1.1637130]

Silicon nanocrystals embedded in SiO₂ exhibit strong room-temperature luminescence, and it is well known that both the luminescence intensity and lifetime can be increased by annealing in molecular hydrogen.^{1–7} This is attributed to hydrogen passivation of competing nonradiative defect centers, such as Si dangling bonds located at the nanocrystal surface. The class of dangling bond defects known as P_b centers is thought to be the dominant recombination site,⁸ and it has been shown that one such defect is sufficient to quench the visible luminescence of a Si nanocrystal.⁹ However, work by Gheorghita *et al.* revealed two further classes of defects at (111) Si/SiO₂ interfaces: one that can be passivated with H₂ (labeled R), and one that cannot.¹⁰

Passivation is usually achieved by thermal annealing of the nanocrystals in forming gas (H₂/N₂), although ion implantation of hydrogen or deuterium with subsequent thermal treatment can be used to similar effect.^{1,3} It is also interesting to note that significant amounts of atomic hydrogen can be generated within an oxide layer if chemically active metals such as Al or Cr are deposited on the surface prior to annealing.¹¹ For planar Si/SiO₂ interfaces this process is known to provide better interface passivation than H₂ ambient annealing, with dangling bond densities on the order of 10¹⁰ cm⁻² eV⁻¹ achievable.¹² When Al is used, this process is sometimes known as an aneal. The aneal has not been applied to the passivation of nanocrystals, although it is commonly used in solar cell fabrication to reduce the surface recombination velocity.¹³ H is believed to be generated by the reaction of water vapor adsorbed at the SiO₂ surface with the deposited Al.¹⁴

In this study, 400 keV Si⁺ ions were implanted into 1.25 μm SiO₂ layers grown on B-doped (0.1–0.3 Ω cm) Czochralski (100) Si by wet thermal oxidation at 1100 °C. The implant fluence was 2 × 10¹⁷ cm⁻², corresponding to a peak excess Si concentration of 10 at. % at a mean projected range of 630 nm.¹⁵

Nucleation and growth of nanocrystals was achieved by annealing the implanted samples at 1100 °C for 1 h in high-purity (99.997%) Ar. Molecular hydrogen passivation was achieved by thermal annealing in high-purity (99.98%) forming gas (5% H₂ in N₂) for times ranging from 1 min to 16 h. A rapid thermal processor (AET Thermal RX) was used for

annealing times ≤ 10 min, with longer anneals performed in a conventional tube furnace. The anneal process consisted of evaporating a 100 nm layer of Al onto the oxide surface prior to a 1 h anneal at 500 °C in forming gas. The Al layer was subsequently removed by etching in 90 °C H₃PO₄ (85%) for 1 min. For consistency, the nonmetallized samples were also subjected to the hot H₃PO₄ etch after the forming gas anneal. The etch was found to have no effect on the photoluminescence (PL).

PL measurements were performed at room temperature, using the 488 nm line of an Ar⁺ laser as the excitation source. Emitted light was analyzed using a single-grating monochromator (TRIAx-320) and detected with a liquid-nitrogen-cooled, front-illuminated, open-electrode CCD array (EEV CCD30-11). All spectra were corrected for system response. Time-resolved PL (TRPL) measurements were performed by modulating the laser beam with an acousto-optic modulator (Brimrose TEM-85-10). A room-temperature multi-alkali photomultiplier (Hamamatsu R928) was used to detect the light from the exit port of the monochromator with the grating centered at 800 nm (bandpass of 40 nm). The signal from the photomultiplier was collected using a digital storage oscilloscope. The timing resolution of the system is < 1 μs.

Figure 1 shows the effect of hydrogen passivation on the nanocrystal PL. There is a significant increase in the PL intensity after annealing in forming gas at 500 °C for 1 h.

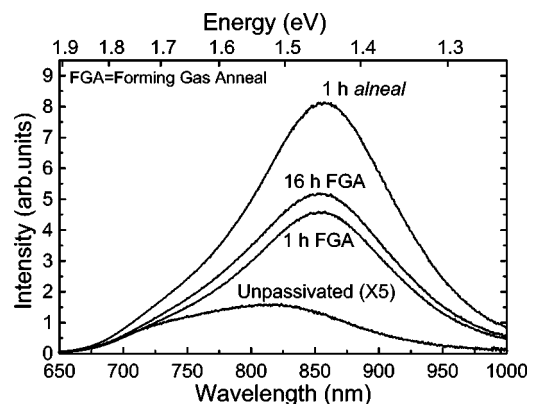


FIG. 1. PL spectra of Si nanocrystals showing the effect of hydrogen passivation. The passivation anneals were performed at 500 °C. The unpassivated spectrum is multiplied by a factor of 5 for clarity.

^{a)}Electronic mail: arw109@rshysse.anu.edu.au

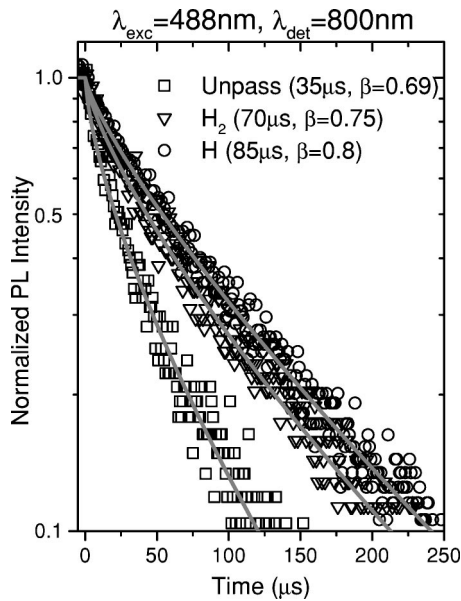


FIG. 2. PL decay traces from TRPL measurements with stretched exponential fits [Eq. (1)]. The values determined for τ and β are indicated on the figure.

These annealing conditions have previously been shown to be optimal for maximizing the PL intensity.⁸ Extending the annealing time to 16 h results in only a small increase in intensity over the 1 h anneal. In contrast, by simply evaporating a layer of Al on the oxide surface before annealing in forming gas, a much greater increase in intensity and lifetime can be achieved.

Despite the significant increase in the level of passivation, Fig. 1 shows that there is no significant redshift relative to that of samples annealed in forming gas. This is in contrast to the initial redshift relative to the unpassivated sample observed for both the forming gas and alneal samples. Such behavior suggests that passivation may involve more than one class of defects.¹⁰ However, further work is required to confirm such a model.

TRPL can be used to extract the luminescence rise and decay lifetimes by modulating the excitation source. The nanocrystal luminescence decay is characterized by a stretched exponential shape, given by

$$I(t) = I_0 \exp\left[-\left(\frac{t}{\tau}\right)^\beta\right], \quad (1)$$

where $I(t)$ and I_0 are the intensities as a function of time and at $t=0$, respectively.^{16,17} τ and β are both wavelength dependent and are, respectively, the lifetime and a dispersion factor whose value is a measure of the interaction strength among Si nanocrystals.

Figure 2 shows results from the TRPL measurements. Both τ and β were found to increase with improved passivation. τ can be approximated by $\tau^{-1} = \tau_R^{-1} + \tau_{NR}^{-1}$, where τ_R is the nanocrystal radiative lifetime and τ_{NR} is the nonradiative lifetime. The nonradiative contribution is associated with defects and/or exciton energy migration. Consequently, as defects, which act as fast nonradiative recombination states, are inactivated, τ_{NR} increases and τ approaches τ_R . Furthermore, the nanocrystals become more isolated due to the re-

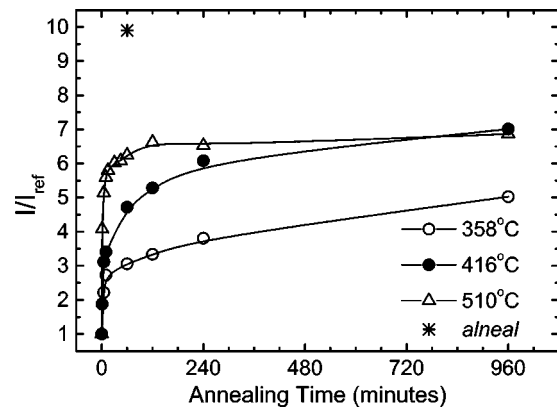


FIG. 3. PL intensity at 800 nm relative to the reference sample (unpassivated), for samples annealed in forming gas at 358, 416, and 510 °C, and after the alneal process. The solid lines are provided as a guide to the eye only.

duction in exciton migration channels. This is consistent with the observed increase in τ and β as the degree of passivation improves.

Figure 3 shows the PL intensity normalized to the unpassivated sample from isothermal annealing sequences at three temperatures in forming gas. Along with this data, is that obtained from the 1 h alneal process. The intensity is taken from the TRPL measurements at 800 nm. This shows that the level of passivation obtainable after a 1 h alneal is not obtainable via annealing in forming gas alone, even after 16 h.

From the enhancements in intensity and lifetime, we can estimate the increase in the number of luminescent nanocrystals. In the low-pump-power regime, the PL intensity of the emitting centers can be approximated by the following expression:¹⁸

$$I = \sigma \phi \frac{\tau}{\tau_R} n^*, \quad (2)$$

where σ is the nanocrystal excitation cross section, ϕ is the photon flux, τ_R is the radiative lifetime, and n^* is the total number of Si nanocrystals that are able to emit. This equation shows that, for constant excitation conditions, a variation in the luminescence yield can only be due to a change in τ , n^* , or both, since τ_R and σ are independent of defect effects. This allows the extraction of the relative n^* from the PL intensity and lifetime.

The enhancements in intensity and lifetime at 800 nm from the alneal compared to forming gas alone are factors of 1.6 and 1.2, respectively. Using Eq. (2), this corresponds to a 30% increase in the number of luminescent nanocrystals over the optimized 1 h forming gas anneal. This enhancement, and the fact that similar levels of passivation cannot be achieved with molecular hydrogen, even after 16 h anneals, implies that a fraction of the nonradiative defects are unable to react with molecular hydrogen. However, electron spin resonance measurements suggest that the structure of the residual defects is the same before and after passivation; only the defect density is affected.^{19,20} The difference in reactivity may therefore simply result from different atomic configurations in the vicinity of the defects, with some defects “steri-

cally protected” from the H₂ molecule but able to react with the smaller H atom.

In summary, Si nanocrystals in SiO₂ have been hydrogen passivated in forming gas and via a post-metallization anneal (alneal). The alneal was found to achieve greater levels of Si nanocrystal passivation, resulting in increased PL intensity compared to standard forming gas annealing. These data were shown to be consistent with the presence of at least two different recombination centers at the nanocrystal/SiO₂ interface: one that reacts with molecular hydrogen and one that only reacts with atomic hydrogen. While an extension of this preliminary study is required to fully understand the kinetics of the alneal process, the method clearly allows improved passivation to be achieved with little extra processing over the standard passivation process for Si nanocrystals.

The authors acknowledge financial support from the Australian Research Council.

¹K. S. Min, K. V. Shcheglov, C. M. Yang, H. A. Atwater, M. L. Brongersma, and A. Polman, *Appl. Phys. Lett.* **69**, 2033 (1996).

²E. Neufeld, S. Wang, R. Apetz, Ch. Buchal, R. Carius, C. W. White, and D. K. Thomas, *Thin Solid Films* **294**, 238 (1997).

- ³S. P. Withrow, C. W. White, A. Meldrum, J. D. Budai, D. M. Hembree, Jr., and J. C. Barbour, *J. Appl. Phys.* **86**, 396 (1999).
- ⁴S. Cheylan and R. G. Elliman, *Nucl. Instrum. Methods Phys. Res. B* **148**, 986 (1999).
- ⁵S. Cheylan and R. G. Elliman, *Nucl. Instrum. Methods Phys. Res. B* **175–177**, 422 (2001).
- ⁶S. Cheylan and R. G. Elliman, *Appl. Phys. Lett.* **78**, 1912 (2001).
- ⁷S. Cheylan and R. G. Elliman, *Appl. Phys. Lett.* **78**, 1225 (2001).
- ⁸A. R. Wilkinson and R. G. Elliman, *Phys. Rev. B* **68**, 155302 (2003).
- ⁹M. Lannoo, C. Delerue, and G. Allan, *J. Lumin.* **70**, 170 (1996).
- ¹⁰L. Gheorghita and E. Ogryzlo, *J. Appl. Phys.* **87**, 7999 (2000).
- ¹¹R. F. Pierret, *Field Effect Devices*, 2nd ed. (Addison-Wesley, Reading, MA, 1990), p. 109.
- ¹²S. K. Ghandhi, *VLSI Fabrication Principles: Silicon and Gallium Arsenide*, 2nd ed. (Wiley, New York, 1994), p. 478.
- ¹³M. J. Kerr and A. Cuevas, *Semicond. Sci. Technol.* **17**, 35 (2002).
- ¹⁴M. L. Reed and J. D. Plummer, *J. Appl. Phys.* **63**, 5776 (1988).
- ¹⁵J. F. Ziegler, J. P. Biersack, and U. Littmark, *The Stopping and Range of Ions in Solids* (Pergamon, New York, 1985).
- ¹⁶L. Pavesi, and M. Cescini, *Phys. Rev. B* **48**, 17625 (1993).
- ¹⁷J. Linnros, A. Galeckas, N. Lalic, and V. Grivickas, *Thin Solid Films* **297**, 167 (1997).
- ¹⁸D. Pacifici, E. C. Moreira, G. Franzò, V. Martorino, and F. Priolo, *Phys. Rev. B* **65**, 144109 (2002).
- ¹⁹A. Stesmans, *J. Appl. Phys.* **88**, 489 (2000).
- ²⁰M. López, B. Garrido, C. García, P. Pellegrino, A. Pérez-Rodríguez, J. Morante, C. Bonafos, M. Carrada, and A. Claverie, *Appl. Phys. Lett.* **80**, 1637 (2002).